

RESEARCH

Open Access



Computational wear of knee implant polyethylene insert surface under continuous dynamic loading and posterior tibial slope variation based on cadaver experiments with comparative verification

Alaettin Ozer*

Abstract

Background: The effect of posterior tibial slope on the maximum contact pressure and wear volume of polyethylene (PE) insert were not given special attention. The effects of flexion angle, Anterior-Posterior (AP) Translation, and Tibial slope on the max contact pressure and wear of PE insert of TKR were investigated under loadings which were obtained in cadaver experiments by using Archard's wear law. This study uses not only loads obtained from cadaver experiments but also dynamic flexion starting from 0 to 90 degrees.

Method: Wear on knee implant PE insert was investigated using a 2.5 size 3 dimensional (3D) cruciate sacrificing total knee replacement model and Finite Element Method (FEM) under loadings and AP Translation data ranging from 0 to 90 flexion angles validated by cadaver experiments. Two types of analyses were done to measure the wear effect on knee implant PE insert. The first set of analyses included the flexion angles dynamically changing with the knee rotating from 0 to 90 angles according to the femur axis and the transient analyses for loadings changing with a certain angle and duration.

Results: It is seen that the contact pressure on the PE insert decreases as the cycle increases for both Flexion and Flexion+AP Translation. It is clear that as the cycle increases, the wear obtained for both cases increases. The loadings acting on the PE insert cannot create sufficient pressure due to the AP Translation effect at low speeds and have an effect to reduce the wear, while the effect increases with the wear as the cycle increases, and the AP Translation now contributes to the wear at high speeds. It is seen that as the posterior tibial slope angle increases, the maximum contact pressure values slightly decrease for the same cycle.

Conclusions: This study indicated that AP Translation, which changes direction during flexion, had a significant effect on both contact pressure and wear. Unlike previous similar studies, it was seen that the amount of wear continues to increase as the cycle increases. This situation strengthens the argument that loading and AP Translation values that change with flexion shape the wear effects on PE Insert.

Keywords: Total knee replacement, Finite element model, Wear, Posterior Tibial slope, Continuous dynamic loading

*Correspondence: alaettin.ozero@bozok.edu.tr

Department of Mechanical Engineering, Yozgat Bozok University, Yozgat, Turkey



Introduction

Wear is the removal, surface damage, or displacement of material from one or both solid surfaces when it is subjected to contact and relative motion with another body. Operating conditions affect interface wear. The wear of components is often a significant determinant of the product's service life.

Modeling of wear in a computational framework has been previously made effort in order to estimate the amount of PE wear that occurs at the articular surface in total knee replacements (TKR). Most of the wear studies [1–7] have been founded on Archard's law of wear [8] by using a wear factor derived using experiments.

Osteolysis induced by particles is one of the most important reasons that limit the endurance of TKR. It is developed by the wear of bearing components made of ultra-high molecular weight polyethylene (UHMWPE) [9]. Wear can occur on the proximal surface of modular designs [9], as well as the distal surface [10–17], the surface of patella resurfacing components [18], and the post of posterior stabilized designs [9]. Wear particles can trigger an immunological response, which can set off a chain reaction of negative tissue reactions that leads to osteolysis and implant loosening [19].

The purpose of the wear experiments of TKR is to investigate surface bearing and prosthesis. Wear simulators simulate in vivo circumstances, enabling for performance evaluation of innovative designs prior to large-scale production and implantation. Researchers, manufacturers, and industry professionals can use simulator wear testing to evaluate the wear performance of their prosthesis design and bearing materials under physiological conditions. This testing can help to refine and improve their designs prior to large-scale manufacturing and implantation, in addition to meeting regulatory criteria.

Models predict wear have been earning interest within the research community as they are quicker and cheaper than experimental tests and can be easily used to study the effect of different working conditions, which could hardly be reproduced experimentally. The authors have developed some analytical models to predict wear in hip and shoulder implants. However, since they do not take into account the update of the geometry as wear evolves, they can provide useful indications for wear effects only in the short term.

Such limitations can be solved by Finite Element wear models, which are preferred for analytical solutions for simulating wear in long tests and also in cases of complex geometries. However, one of their main limitations is the computational cost. They need repetitive nonlinear contact analysis. But these limitations can be overcome by using realistic simplifications.

To anticipate pressure and wear distribution on the insert surface, Zhang et al. [20] employed a patient-specific lower extremity musculoskeletal multibody dynamics model using FEM.

Kang et al. [21] evaluated the biomechanical impact of various tibial insert materials on knee joints: UHMWPE, poly-ether-ether-ketone (PEEK), and carbon-fiber-reinforced PEEK.

Mell et al. [22] developed a computational methodology for modeling TKR wear using finite element analysis, and studied the effect of femoral center of rotation location on TKR PE wear during standardized displacement controlled testing.

Kawanabe et al. [23] created a simulator for complete knee replacements and investigated the effects of tibial AP Translation and internal-external (IE) rotation on the wear of polyethylene tibial implants. They found that IE rotation, tibial AP Translation, and rolling contributed to the higher wear rate under four types of experiments that have different loadings, suggesting that the tibial UHMWPE suffered more damage as a result of the IE.

On an in vitro knee simulator, Johnson et al. [24] evaluated the relative relevance of tibial IE rotation and femoral AP Translation and determined wear rates for the IB-II knee prosthesis for a complete normal speed walking gait cycle. They proposed that the wear rate of UHMWPE is affected by various factors such as the amount of multidirectional shear motion and the ratio of rolling/sliding contact kinematics, as well as the applied load.

The link between the posterior tibial slope (0, 7, 10 degrees), the contact force, and stresses on the medial and lateral ligaments during knee flexion following posterior-stabilized TKA was studied using FEM by Lee H.Y. et al. [25].

Using 3D finite element modeling, Shen et al. [26] studied the effect of posterior tibial slope on contact stresses in the polyethylene component of total knee prosthesis. The wear behavior of four distinct posterior tibial slopes was examined to determine the best posterior slope.

Using finite element modeling, Koh et al. [27] investigated the impact of the posterior tibial slope in mobile-bearing unicompartmental knee arthroplasty (UKA). They discovered that as the posterior tibial slope increased, contact stress increased, increasing the strain exerted on the ACL.

The effect of posterior tibial slope on the maximum contact pressure and wear volume of PE insert were not given special attention. Thus, in this study, the effects of flexion angle, AP Translation, and Tibial slope on the max contact pressure and wear of PE insert of TKR were investigated under loadings which were obtained in cadaver experiments by using Archard's wear law. This study uses not only loads obtained from cadaver

experiments but also dynamic flexion starting from 0 to 90 degrees.

Materials and methods

Wear model

The Archard wear model is a widely used sliding wear model that produces reasonable results when used with FEM to simulate wear. According to Archard's original model, the contact pressure and sliding velocity at the contact surface are proportional to the rate of volume loss due to wear. The program implements a generalized version of this model that allows correct law dependence on contact pressure and velocity.

Wear is supposed to occur in the surface's inward normal direction, which is the opposite of the contact normal direction. As a result, in Ansys, the rate of wear at a contact node is given by

$$W = \frac{K}{H} P^m V^n$$

Where, K is the wear coefficient, H is the material hardness, P is the contact pressure, V is the relative sliding velocity, m is the pressure exponent and n is the velocity exponent.

Finite element model, analyses, materials, loading

Probably the most important part of a knee implant is the PE Insert which is made up of durable polyethylene material and which functions as meniscus in the knee. While the other pieces are metal parts with generally high solidity, the PE insert is expected to have a structure that is relatively softer, more resistant to wear, and capable of absorbing beats. For this reason, it is manufactured from UHMWPE.

In this study, a 2.5 size 3D knee model obtained from Mikron Makine (Yenimahalle/Ankara/Turkey) was used (Fig. 1). Using this solid model, the Finite Element Structural Model was set up by using tetrahedral higher order solid elements. The smallest element size was 1.5 mm after mesh optimization. One hundred forty-eight thousand eight hundred five elements and two hundred twenty-three thousand sixty-nine nodes were used for the mesh (Fig. 1). Models for analyses were obtained by combining this 3D knee model with solid femur and tibia solid models by means of SpaceClaim Software. In the model matched with femur and tibia, the femur component-femur and tibia component-tibia connection places were considered as completely bonded as in real states. To simulate this, the upper end of the femur component and lower end of the PE insert were fixed. To keep femur comp on the insert while flexion, standard earth gravity was applied. The insert was fixed not to move vertically at the lower end but horizontally to model AP

translation and not to move in all directions at the upper end with displacement boundary conditions (Fig. 1). Due to its continuous and dynamic nature, the contact area between femur component and PE insert was considered as frictional although it changed according to flexion angles. The friction coefficient was taken as 0.04 in line with the previous literature [28].

The following substances and values were used for the model adopted within this study. Regarding the bone properties for Femur and Tibia, the Elasticity Modulus (E) was 16.8 GPa and the Poisson's Ratio (ν) was 0.47. Cobalt-Chromium alloy was used for the femur component (E = 195 GPa, ν = 0.3). UHMWPE was used for PE Insert with E = 685 MPa, ν = 0.47. Titanium alloy (Ti6Al4V) was utilized for Tibia component (E = 110 GPa, ν = 0.3) [28].

Two types of analyses were done to measure the wear effect on knee implant PE insert. The first set of analyses included the flexion angles dynamically changing with the knee rotating from 0 to 90 angles according to the femur axis and the transient analyses for loadings changing with a certain angle and duration. In these analyses, the PE insert was located in such a way to form angles with the femur axis by 0, 3, 5, and 7 degrees, which is named as Posterior Tibial Slope. The stable and dynamic loadings used in these analyses were ones obtained from the literature and the cadaver experiments conducted to identify and prove the loadings exerted on the knee in varying states [29]. These loadings are consisted of stable loadings of 50 N on the femur and 10 N on the hamstring and the quadriceps actuator force linearly increased and reached a force of 600 N at a 90 degrees flexion. The second set of analyses consisted of analyses of wear under the influence of AP Translation changing during flexion in addition to the flexion in the first analyses. AP translation was applied to the PE insert as one-directional displacement. The AP translation values were also adopted from the related literature [30].

In this study, wear coefficient for contacting surfaces were chosen and used as independent of contact pressure and obtained from a multi-directional pin on plate study [31]. Especially, to obtain material removal on PE insert, asymmetric contact is used.

The wear coefficient K can be scaled to simplify modeling such that the translation is not explicitly modeled, but its effect is included in the computation of wear. This significantly reduces the simulation time and effort. More specifically, if a linear dependence of wear rate on the sliding velocity is assumed, the wear coefficient K can be scaled by the sliding velocity. So, this results in the wear rate being linearly dependent upon the sliding velocity without explicitly modeling the sliding. This property is also used in this study to reduce computation time. K was scaled such that only

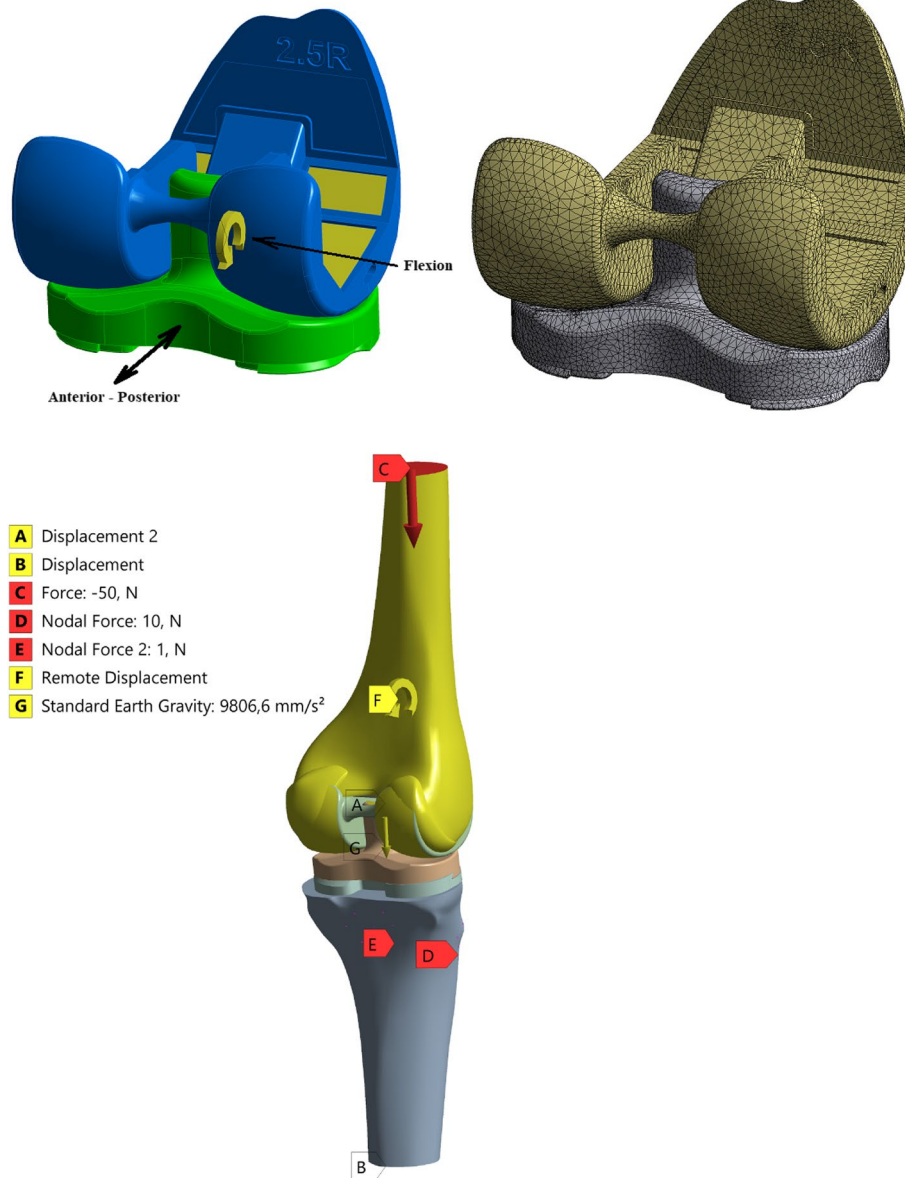


Fig. 1 3D knee implant model (cruciate sacrificing total knee replacement) (upper left), Finite Element Model (upper right) and loading and boundary conditions on model (lower)

distance taken during flexion 0 to 90 degree by femur component contacting with insert until it reaches for example 30 m cycle was scaled. This way reduce time and it is general in wear modeling. AP translation was not scaled with K. It is another boundary condition and modeled as separately.

Ansys Workbench 2020 R2 software was used to set up the Finite Element Models and carry out subsequent data analyses in this study.

Results

Flexion and Flexion + AP Translation

Maximum contact pressure distributions are given for 100 thousand (100k), 1, 3, 10, 20, and 30 million (30m) cycles, respectively in Fig. 2. In addition, the contact pressure distributions show the effect of the AP Translation effect on the PE insert during flexion are also given in Fig. 3. Maximum contact pressure values

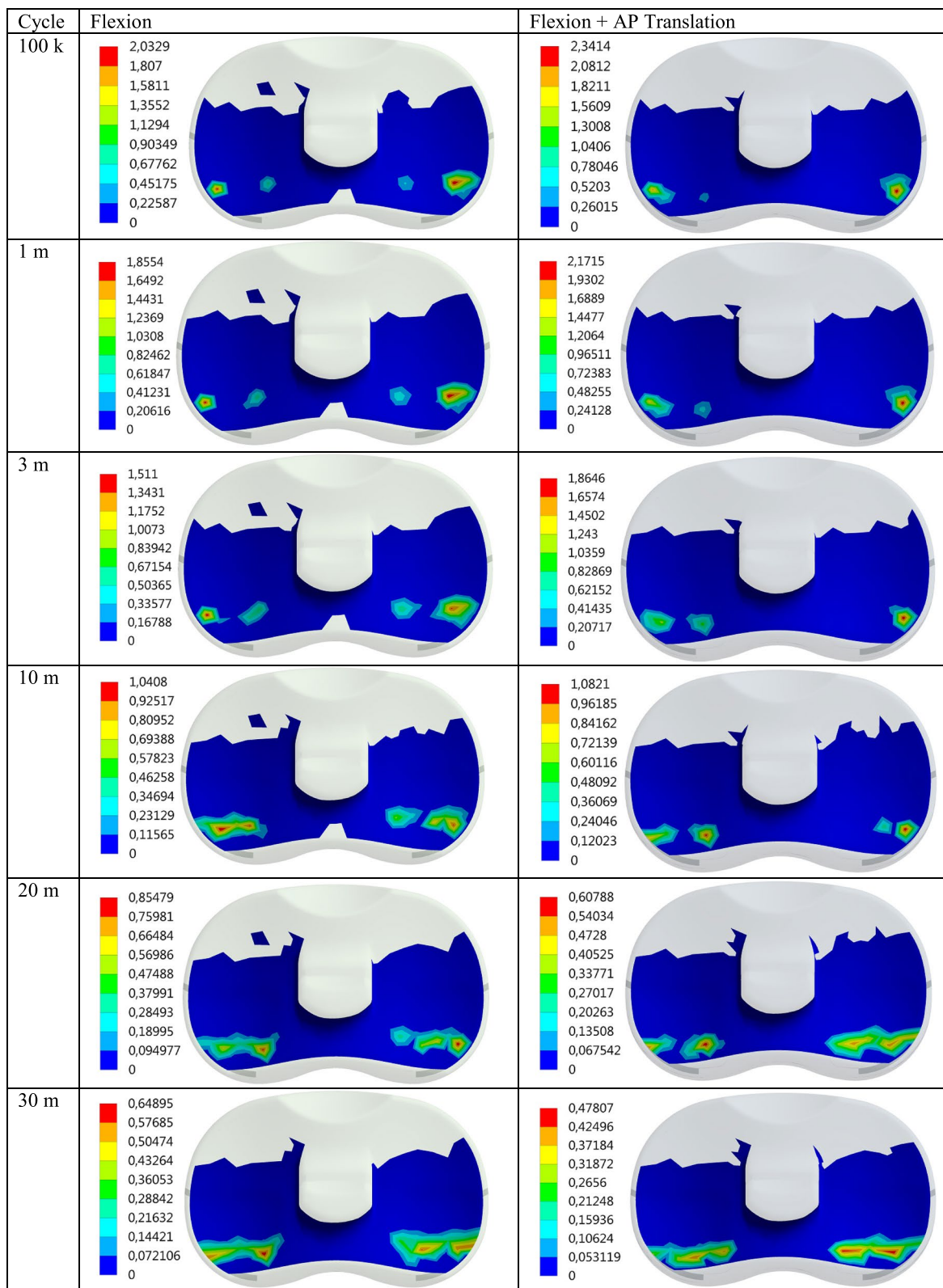


Fig. 2 Max contact pressure distribution (MPa) on the PE insert surface for Flex and Flex+AP Translation wrt cycle

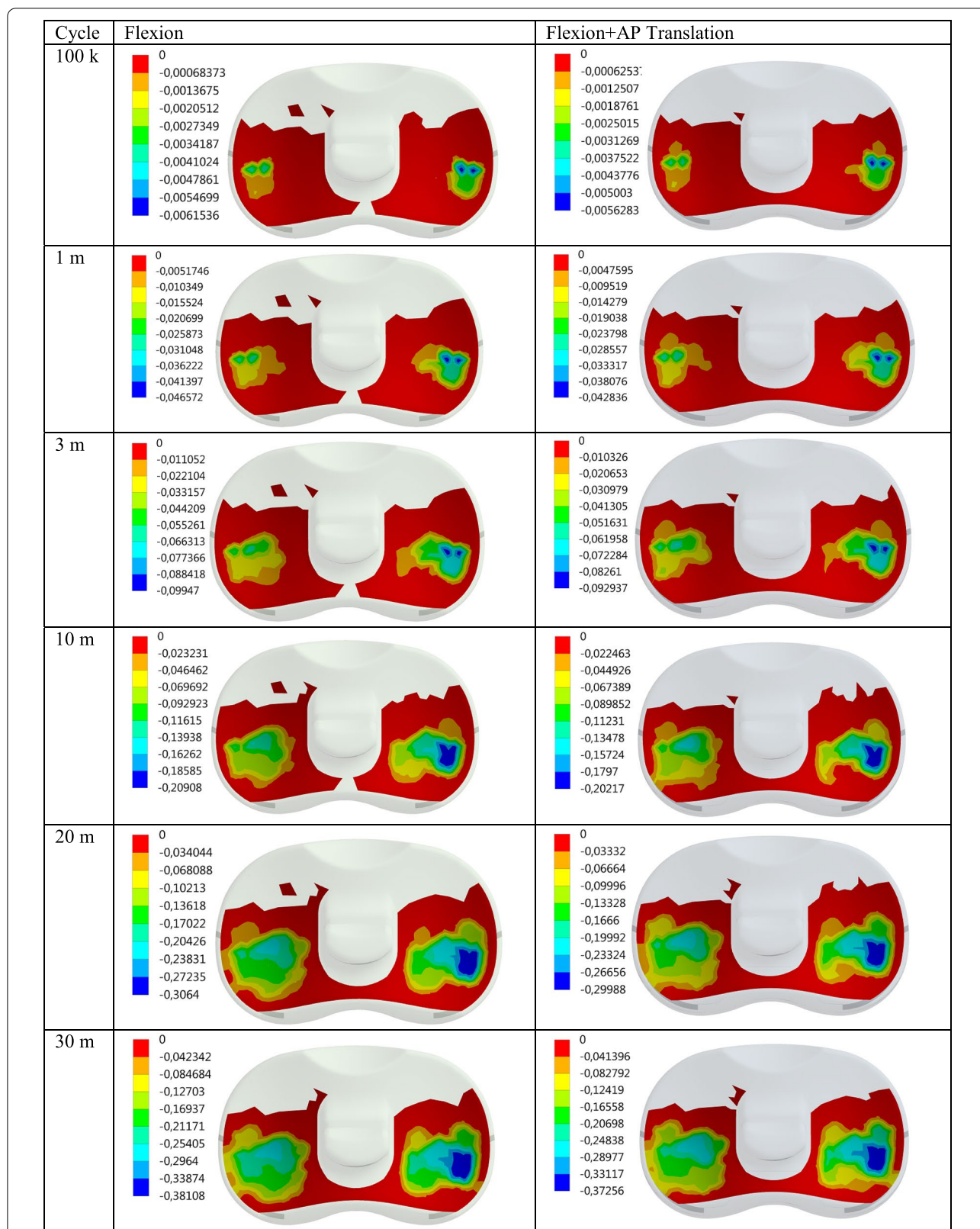


Fig. 3 Wear distribution (mm) on the PE insert surface for Flex and Flex+AP Translation wrt cycle

Table 1 Max contact pressure and wear data for Flexion and Flexion+AP Translation wrt cycle

Cycle	Flexion		Flexion+AP Translation	
	Press (MPa)	Wear (mm)	Press (MPa)	Wear (mm)
100k	2.0329	0.0061536	2.3414	0.0056283
1m	1.8554	0.046572	2.1715	0.042836
3m	1.511	0.09947	1.8646	0.092937
10m	1.0408	0.20908	1.0821	0.20217
20m	0.85479	0.3064	0.60788	0.29988
30m	0.64895	0.38108	0.47807	0.37256

obtained for Flexion and Flexion+AP Translation are given in Table 1 for better interpretation.

It is seen that the contact pressure on the PE insert decreases as the cycle increases for both Flexion and Flexion+AP Translation. Maximum contact pressure values for Flexion and Flexion+AP Translation for 100k cycles were obtained as 2.03 and 2.34 MPa, respectively. Here, while the maximum contact pressure at maximum flexion was 2.03 MPa for 100k cycles, when the cycle was increased 10 times, that is, for 1m cycles, it decreases to 1.86 MPa and the drop rate becomes 1.228. While the increase in the maximum contact pressure caused by the AP Translation, together with the cycles, reaches 1.23 in 3m cycles; when the cycle reaches 10m,

the ratio decreases and it is seen that the contact pressure values for 20-30m cycles are less than the values for flexion only.

When the cycle is 1m, i.e. 100 times the initial rate, the amount of pressure drops by almost half. In the case of flexion only, while the maximum contact pressure is 2.03 MPa for 100k cycles, the pressure drops to 0.65 MPa at 30m. As expected, this can be explained by the increase in wear and the corresponding increase in the contact area as the cycle increases. We can verify this from the increase in the wear corresponding to the cycle (Figs. 4 and 5). While the wear in “only flexion” is 0.006 mm for 100k, this value increases to 0.38 mm at 30m. For Flexion+AP Translation, it increases from 0.0056 mm to 0.37 mm.

It is clear that as the cycle increases, the wear obtained for both cases increases (Fig. 4). In addition, the wear on PE insert in the Flexion only for 100k, 1 million and 3 million cycles are higher than the Flexion+AP Translation and while the initial wear is 1.09, with the increase in the cycles, this rate decreases to 1.02 at 30m.

For Flexion+AP Translation, the pressure value drops from 2.34 MPa to 0.48 MPa. For Flexion+AP, the maximum contact pressure on the PE insert decreases as the cycle increases, just like in Flexion only. It is seen that AP Translation together with flexion increases the contact pressure by approximately 1.15. This shows us that the AP Translation is much more effective as the cycle

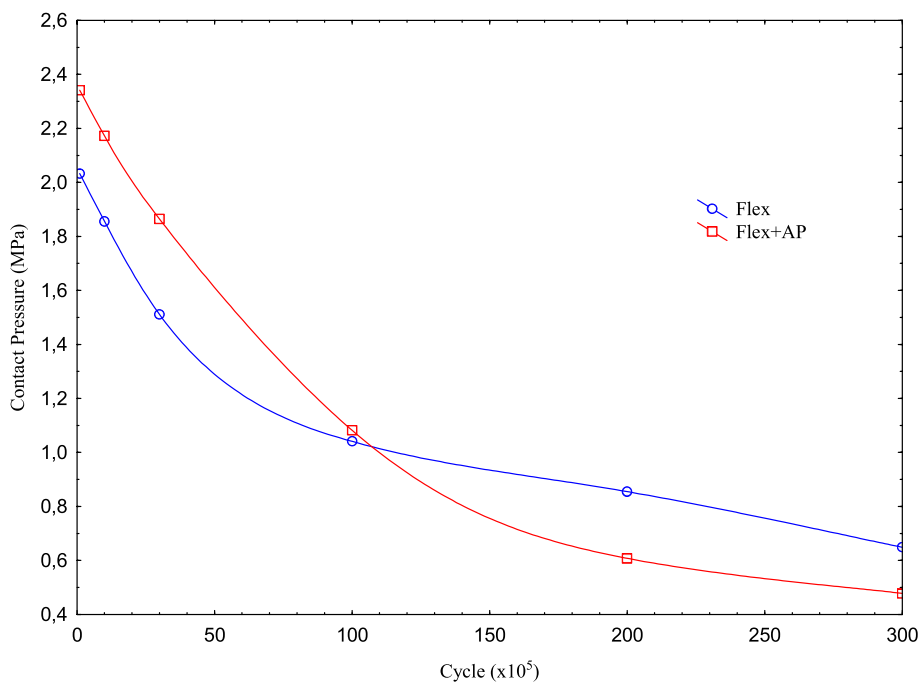
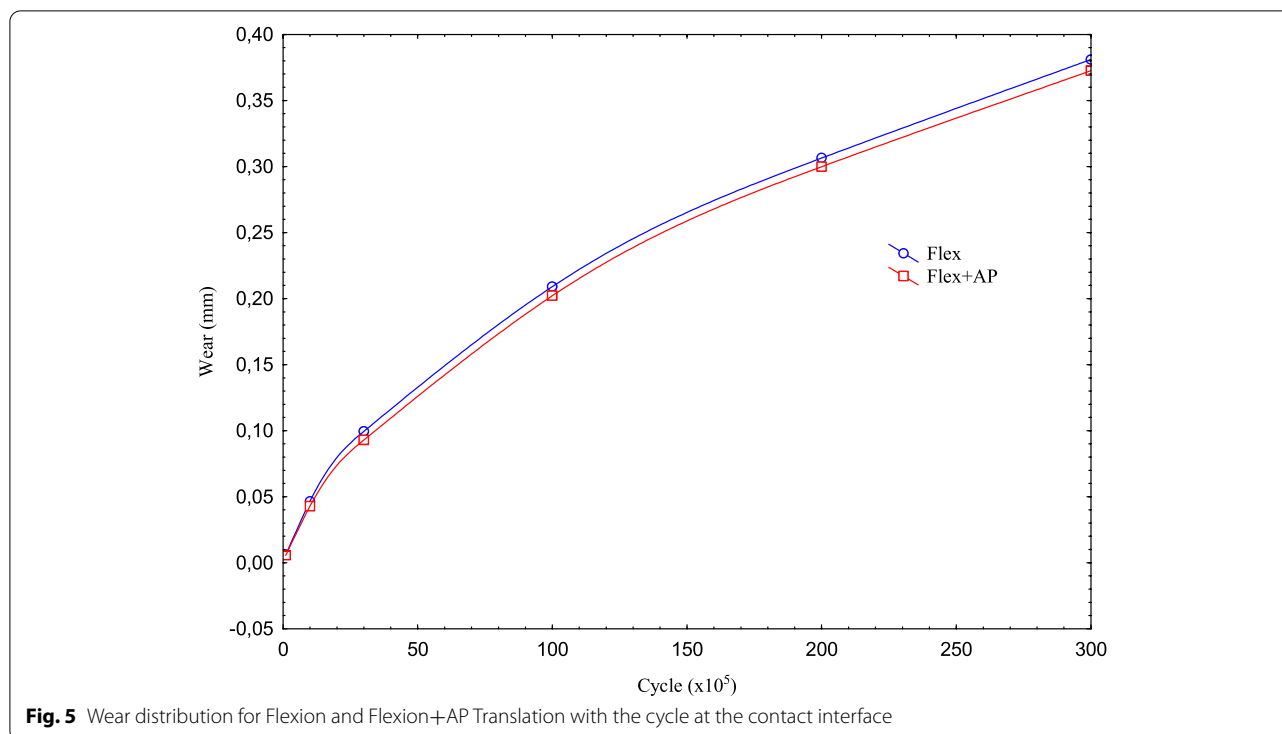


Fig. 4 Max contact pressure distribution for Flexion and Flexion+AP Translation with the cycle at the contact interface



increases tenfold from 10 million onwards. In other words, the loadings acting on the PE insert cannot create sufficient pressure due to the AP Translation effect at low speeds and have an effect to reduce the wear, while the effect increases with the wear as the cycle increases, and the AP Translation now contributes to the wear at high speeds.

Tibial slope

Another concern of this study was to examine the effect of Posterior Tibial slope angle change on the contact surface of the PE Insert in the knee implant, on the maximum pressure distribution and wear, under much more realistic loading obtained by using a cadaver. The pressure and wear distributions obtained after the analyses are given in Figs. 6 and 7 and also in Table 2.

As seen in Table 2, in this study, analyzes were performed for knee implants with the posterior inclination of 3, 5, and 7 degrees in the above-mentioned loading condition for 6 different cycles under dynamic flexion varying between 0 and 90 degrees in increments of 5 degrees each. As seen in Fig. 8, the maximum contact pressure distributions on the PE insert obtained as a result of the analyses performed for the knee implant with a tibial slope of 3, 5 and 7 degrees decrease as the cycle increases. On the other hand, the wear increases as seen in Fig. 9.

It is seen that as the posterior tibial slope angle increases, the maximum contact pressure values slightly decrease for the same cycle. In other words, while the contact pressure is 2.0316 MPa for 100k cycles and 3 degrees; for 5 degrees, this value is 2.0295 MPa, for 7 degrees it is 2.0264 MPa. Although this situation becomes somewhat irregular as the cycle increase, it shows that the trend is not deteriorated in general. On the other hand, it is seen that while the wear increases as the cycle increases for each tibial slope, it decreases as the tibial slope increases for each cycle. In other words, the pressure values obtained for 100k are 2.0316 MPa, 2.0295 MPa, and 2.0264 MPa for the tibial slope of 3, 5, and 7 degrees; the wear decreases in the same angle order. As seen in Fig. 9, while the upward trend in the amount of wear was close until 3 m cycles, the amount of increase went up after this period.

It is seen that the contact pressure decreases, though with small differences, as the Tibial slope angle increases for 100 k, 1 m, and 3 m cycles. For 5 degrees Tibial slope, the contact pressure at 10 m cycles is less than other angles while it is the same for the other angles. In the analyses made for 20 m, it is seen that the pressure tends to decrease again with the increase in angle. In the pressure values obtained for 30 m, a result similar to the result in 10 m cycles was obtained. That is, the pressure value obtained for 5 degrees was higher than the other angles, while the value obtained

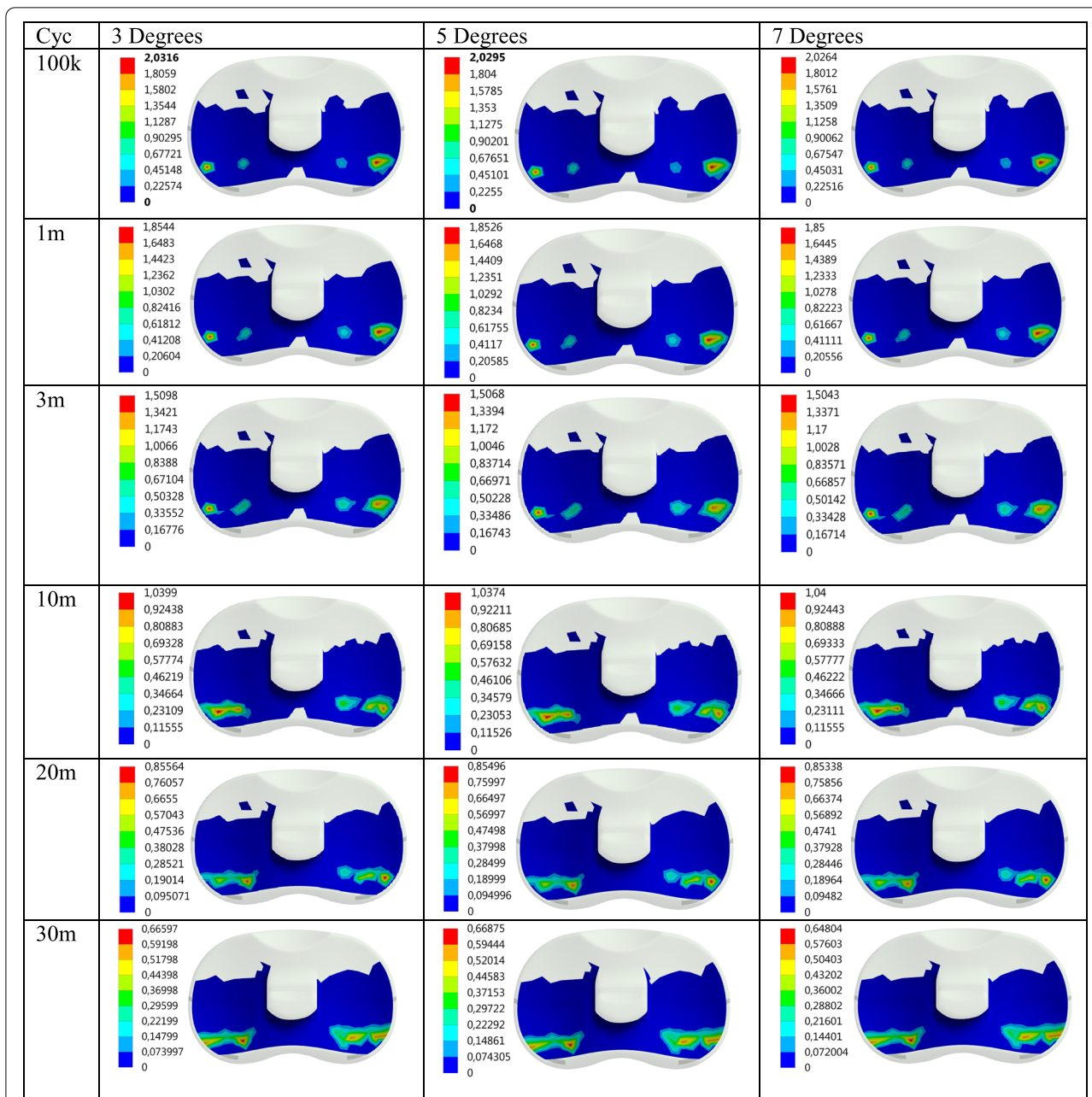


Fig. 6 Max contact pressure distribution (MPa) on the PE insert surface for Posterior Tibial Slope degree wrt cycle

for 7 degrees was the lowest. On the other hand, the wear increases as the cycle increases for each angle. While this upward trend is high at the beginning, it decreases as the cycle increases. However, as the Tibial slope angle increases with the cycles, it is seen that the wear decreases slightly.

Discussion

As expected, the maximum contact pressure value for both analyzes decreases as the number of rotations increases. However, for both types of analysis, this decrease in pressure was very close up to 3m cycles, while the decrease became more stable in the absence

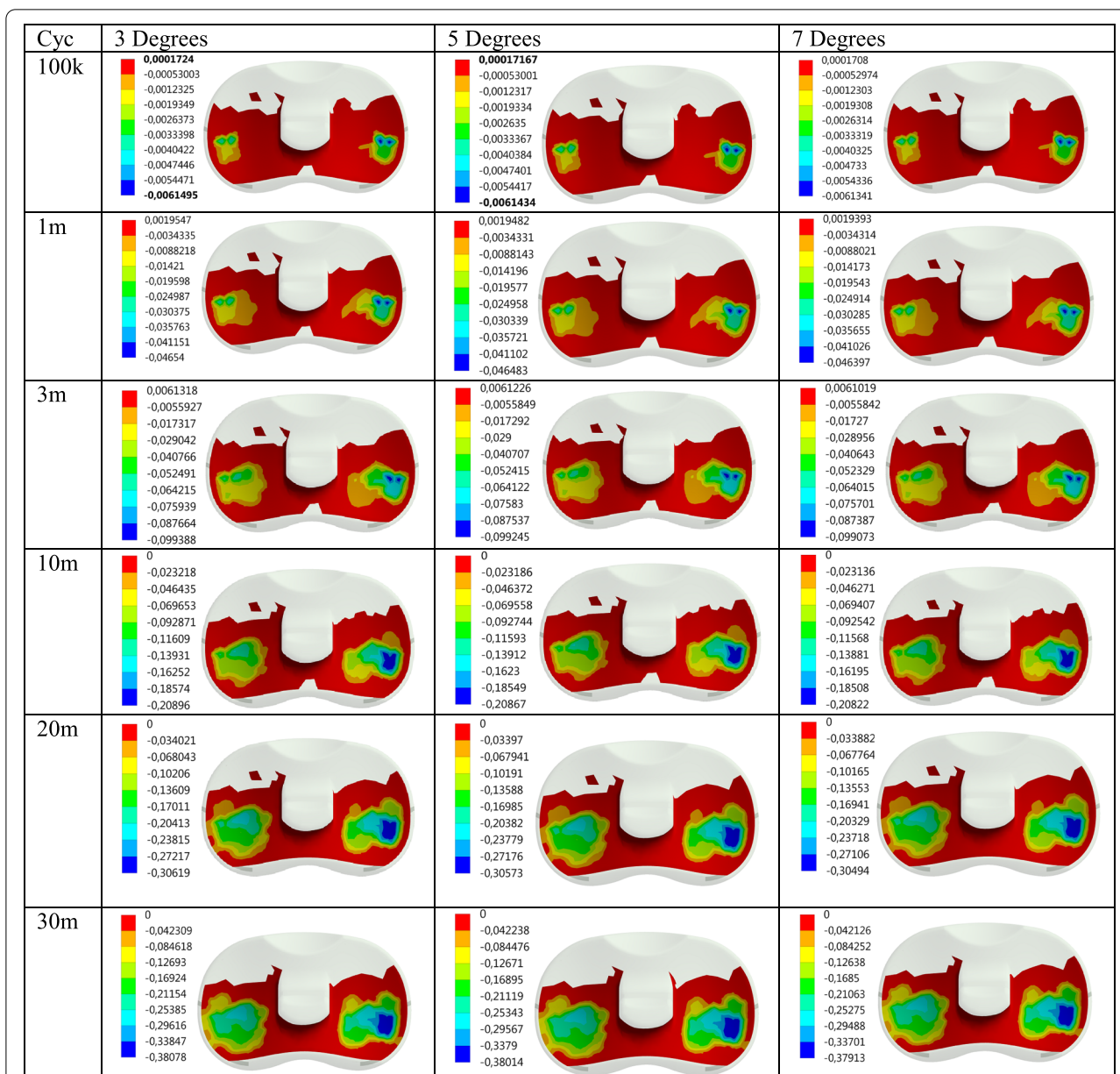
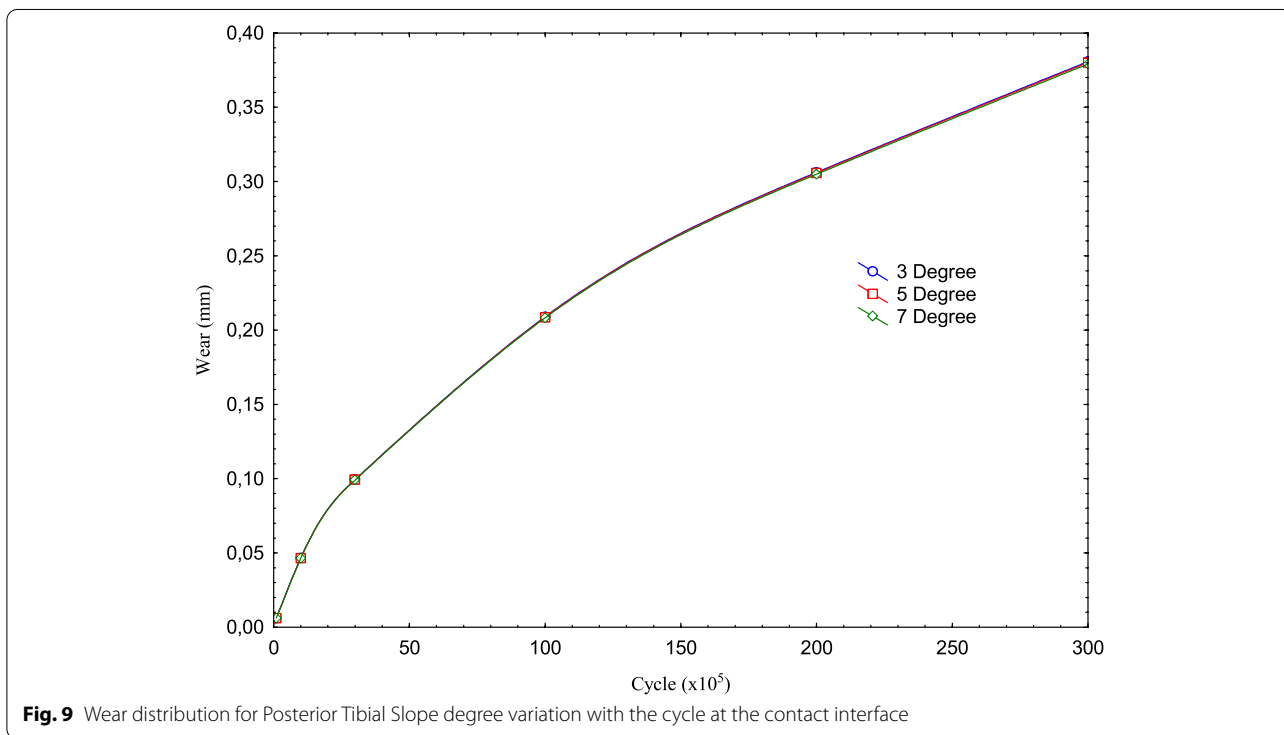
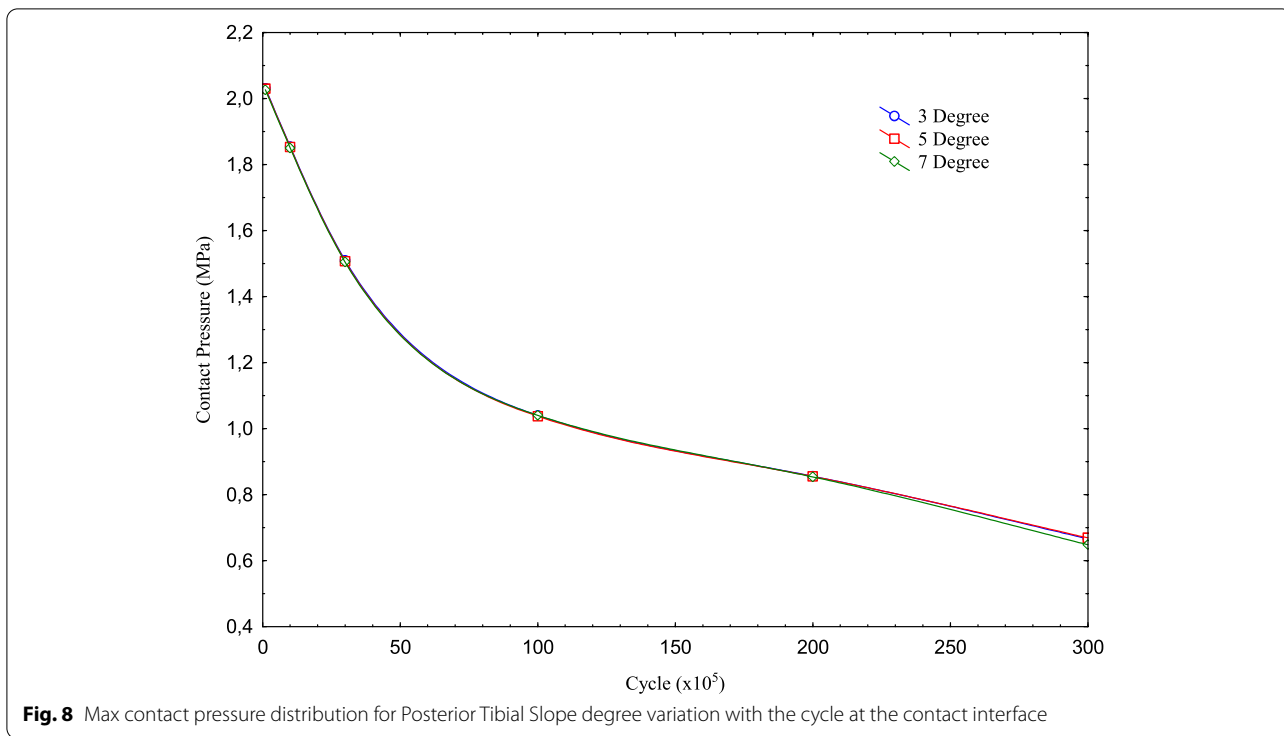


Fig. 7 Wear distribution (mm) on the PE insert surface for Posterior Tibial Slope degree wrt cycle

Table 2 Max contact pressure and wear data for Posterior Tibial Slope degree variation wrt cycle

Cycle	(Tibial Slope) Flexion					
	3 Degrees		5 Degrees		7 Degrees	
	Press (MPa)	Wear (mm)	Press (MPa)	Wear (mm)	Press (MPa)	Wear (mm)
100k	2.0316	0.0061495	2.0295	0.0061434	2.0264	0.0061341
1 m	1.8544	0.04654	1.8526	0.046483	1.85	0.046397
3 m	1.5098	0.099388	1.5068	0.099245	1.5043	0.099073
10m	1.0399	0.20896	1.0374	0.20867	1.04	0.20822
20m	0.85564	0.30619	0.85496	0.30573	0.85338	0.30494
30m	0.66597	0.38078	0.66875	0.38014	0.64804	0.37913



of AP Translation at 10m. The slope in the AP Translation showed itself up to 20m cycles. After 20m cycles, the decreasing slopes continued close to each other. The

fact that the pressure continued to decrease at almost the same slope as the cycle after 3m cycles could be explained as the effect of AP Translation. The stabilization of the

maximum pressure due to the effect of AP Translation took effect after 20m cycles.

For both types of analysis, the wear, as was the case in maximum pressure distribution, had a similar trend up to 3m cycles and the values were close to each other. After this period, the wear increase trends decreased for both analyzes. The decreasing trends of the analyzes remained almost the same as the number of cycles increased. On the other hand, there is some difference in the wear. Although the AP Translation increases the maximum contact pressure at low speeds and decreases it at high speeds, in this study, the wear is reduced by small amounts after 1m cycles. As given in Wünschel et al. [30], the AP Translation data changes direction depending on the flexion angle. This shift of direction changes the nature of the problem according to the loading condition where only the Femur Component rotates according to flexion.

Now, while the femoral component rotates on the insert, the insert also makes a sliding motion in the AP direction in contact with the femoral component. This causes a difference in both the maximum contact pressure distribution and the wear distribution compared to the other model. It has been stated in previous studies that the rotational movement of the femur component on the insert due to flexion with respect to the femoral axis includes both rolling and slipping, whereas slipping is dominant in this movement [32, 33]. In addition, the AP Translation causes additional sliding motion. This additional movement, especially after 3m cycles, prevents the transfer of the loading causing wear to the contact area, resulting in the amount of wear to be slightly lower. It causes the maximum contact pressure to occur in the left region. However, the maximum wear continues to take place in the right region.

Although the AP Translation initially increased the pressure a little and decreased the wear, it had an effect on reducing the pressure and still reducing the amount of wear in 10m and higher cycles. This can be explained by the fact that AP Translation up to 10m effectively increases the slip, thereby reducing the loading effect on the insert. In other words, it causes the loading to act on a smaller area and the pressure to be higher. However, at high cycles, this effect diminishes and the contact area increases while the pressure decreases. On the other hand, the lower wear can be attributed to the larger wear area.

As given in the Results section, as the cycle increases for each Posterior Tibial slope angle, the maximum contact pressure on the PE insert decreases and accordingly the wear increases. However, it is seen that the wear decreases as the posterior tibial slope angle increases with increasing cycles. This is because as the angle

increases, one of the 50 Newtons force on the connection interface is still perpendicular to the contact interface while the other is divided into two forces that start to act parallel to the contact interface and the one perpendicular to the contact interface decreases and the parallel one increases. In other words, while the perpendicular force is 49.93N for an angle of 3 degrees, it decreases to 49.81 for 5 degrees and 49.63N at 7 degrees. On the other hand, the force parallel to the contact interface is 2.62, 4.36, and 6.09N for 3, 5, and 7 degrees, respectively.

The loading used in this study shows that as the cycle increases for AP Translation and AP Tibial slope angle, the wear area on the PE insert enlarges and approaches the Posterior. While this situation is not very evident in relatively low cycles such as 100k and 1m, it becomes evident in cycles such as 20m and 30m. This can be because the knee implant used in this study is a model called cruciate sacrificing total knee replacement. In this model, as the femoral component rotates with flexion, after a certain angle, it touches the projection designed to function as the posterior cruciate ligament on the PE insert and erodes this region more.

The slight decrease in the wear with posterior tibial slope angle is due to the fact that the vertical loading force, which is perpendicular to the PE insert-Femur Component interface at 0 degree and taken as 50N in this study, splits into two components as perpendicular and parallel to the contact interface as the mounting angle changes, and that the parallel force increases and the perpendicular force decreases as the angle increases. In addition, it is seen as an advantage to use a bigger angle in the knee implant since the wear is reduced as the mounting angle, i.e. the Posterior Slope angle increases. On the other hand, although using a bigger angle is seen as an advantage, as the angle increases, the force acting parallel to the contact interface will increase, forcing the interface to slide even in the static state. For this reason, it will be useful to carry out additional experimental and numerical studies to determine the static and dynamic nature of the Posterior Slope angle change together with the direction of the forces coming to the interface, flexion, AP Translation, and other factors.

This study demonstrated that the wear distributions (based on cycle) drawn according to the data obtained as a result of the simulations were qualitatively similar to the experimental studies conducted by Kawanabe et al. [23]. These findings also revealed that the correct result was obtained depending on the selected wear model. In addition, although the loading inputs were different, the wear amount distributions were qualitatively similar to the numerical study of Zhang et al. [20] up to 15k cycles. On the other hand, unlike previous studies, the wear was found to continue to increase as the number of cycles

increased, although the slope decreased. It was found that the wear zone on the PE insert was obtained as a result of this study and the change with the cycle of this zone were in parallel with the “change of wear zones according to the number of rotations on the insert” obtained by Zhang et al. [20] who used a wear model from the literature.

Conclusions

This study was limited in that it does not take into account tibial rotation and indicated that AP Translation, which changes direction during flexion, had a significant effect on both contact pressure and wear. Unlike previous similar studies, it was seen that the amount of wear continues to increase as the cycle increases. This situation strengthens the argument that loading and AP Translation values that change with flexion shape the wear effects on PE Insert. It is seen that the posterior tibial slope angle - which occupies an important place in the amount of wear on the insert and the load coming to the contact interface in the knee implant mounting - increases with the cycles, and the wear slightly decreases.

Acknowledgments

Not applicable.

Author's contributions

Alaettin OZER has made, generated, and analyzed all data and written the manuscript during this study. The author(s) read and approved the final manuscript.

Funding

Not applicable.

Availability of data and materials

All data generated or analyzed during this study are included in this manuscript.

Declarations

Ethics approval and consent to participate

This study was approved by Mikron Makine (Yenimahalle/Ankara/Turkey).

Consent for publication

Not applicable.

Competing interests

The authors declare that they have no competing interests.

Received: 15 March 2022 Accepted: 14 September 2022

Published online: 19 September 2022

References

- Knight LA, Pal S, Coleman JC, Bronson F, Haider H, Levine DL, et al. Comparison of long-term numerical and experimental total knee replacement wear during simulated gait loading. *J Biomech*. 2007;40:1550–8.
- Barbour PSM, Barton DC, Fisher J. The influence of contact stress on the wear of UHMWPE for total replacement hip prostheses. *Wear*. 1995;181–183:250–7.
- Fregly BJ, Sawyer WG, Harman MK, Banks SA. Computational wear prediction of a total knee replacement from in vivo kinematics. *J Biomech*. 2005;38:305–19.
- Maxian TA, Brown TD, Pedersen DR, Callaghan JJ. A sliding-distance-coupled finite element formulation for polyethylene wear in total hip arthroplasty. *J Biomech*. 1996;29:687–92.
- Pal S, Haider H, Laz PJ, Knight LA, Rullkoetter PJ. Probabilistic computational modeling of total knee replacement wear. *Wear*. 2008;264:701–7.
- Zhao D, Sakoda H, Sawyer WG, Banks SA, Fregly BJ. Predicting knee replacement damage in a simulator machine using a computational model with a consistent wear factor. *J Biomech Eng*. 2008;130:011004–10.
- Zhao D, Sawyer W, Fregly B. Computational wear prediction of UHMWPE in knee replacements. *J ASTM Int*. 2006;3:45–50.
- Archard JF. Contact and rubbing of flat surfaces. *J Appl Phys*. 1953;24(8):981–8.
- Kurtz S. UHMWPE biomaterials handbook: ultra high molecular weight polyethylene in total joint replacement and medical devices. Amsterdam: Elsevier/Academic Press; 2009.
- Akisue T, Yamaguchi M, Bauer TW, Takikawa S, Schils JP, Yoshiya S, et al. “Backside” polyethylene deformation in total knee arthroplasty. *J Arthroplasty*. 2003;18:784–91.
- Azzam MG, Roy ME, Whiteside LA. Second-generation locking mechanisms and ethylene oxide sterilization reduce tibial insert backside damage in total knee arthroplasty. *J Arthroplasty*. 2011;26:523–30.
- Brandt JM, MacDonald SJ, Bourne RB, Medley JB. Retrieval analysis of modular total knee replacements: factors reducing backside surface damage. *Knee*. 2012;19(4):306–15.
- Condit MA, Ismaili SK, Alexander JW, Noble PC. Backside wear of modular ultra-high molecular weight polyethylene tibial inserts. *J Bone Joint Surg Am*. 2004;86:1031–7.
- Engh GA, Koralewicz LM, Perles TR. Clinical results of modular polyethylene insert exchange with retention of total knee arthroplasty components. *J Bone Joint Surg Am*. 2000;82:516.
- Engh GA, Lounici S, Rao AR, Collier MB. In vivo deterioration of tibial baseplate locking mechanisms in contemporary modular total knee components. *J Bone Joint Surg Am*. 2001;83:1660–5.
- O'Rourke MR, Callaghan JJ, Goetz DD, Sullivan PM, Johnston RC. Osteolysis associated with a cemented modular posterior-cruciate-substituting total knee design: five to eight-year follow-up. *J Bone Joint Surg Am*. 2002;84:1362–71.
- Wasielowski RC, Parks N, Williams I, Surprenant H, Collier JP, Engh G. Tibial insert undersurface as a contributing source of polyethylene wear debris. *Clin Orthop Relat Res*. 1997;345:53–9.
- Puloski SKT, McCalden RW, MacDonald SJ, Rorabeck CH, Bourne RB. Tibial post wear in posterior stabilized total knee arthroplasty. An unrecognized source of polyethylene debris. *J Bone Joint Surg Am*. 2001;83:390–7.
- Jasty M, Floyd W, Schiller A, Goldring S, Harris W. Localized osteolysis in stable, non-septic total hip replacement. *J Bone Joint Surg Am*. 1986;68:912–9.
- Zhang J, Chen Z, Wang L, Li D, Jin Z. A patient-specific wear prediction framework for an artificial knee joint with coupled musculoskeletal multi-body-dynamics and finite element analysis. *Tribol Int*. 2017;109:382–9.
- Kang KT, Son J, Kwon SK, Kwon O-R, Park J-H, Koh Y-G. Finite element analysis for the biomechanical effect of tibial insert materials in total knee arthroplasty. *Compos Struct*. 2018;201:141–50.
- Mell SP, Wimmer MA, Lundberg HJ. The choice of the femoral center of rotation affects material loss in total knee replacement wear testing - a parametric finite element study of ISO 14243-3. *J Biomech*. 2019;88:104–12.
- Kawanabe K, Clarke IC, Tamura J, Akagi M, Good VD, Williams PA, et al. Effects of A–P translation and rotation on the wear of UHMWPE in a total knee joint simulator. *J Biomed Mater Res Part B*. 2001;54(3):400–6.
- Johnson TS, Laurent MP, Yao JQ, Gilbertson LN. The effect of displacement control input parameters on tibiofemoral prosthetic knee wear. *Wear*. 2001;250:222–6.
- Lee HY, Kim SJ, Kang KT, Kim SH, Park KK. The effect of tibial posterior slope on contact force and ligaments stresses in posterior-stabilized total knee arthroplasty-explicit finite element analysis. *Knee Surg Relat Res*. 2012;24(2):91–8.

26. Shen Y, Li X, Fu X, Wang W. A 3D finite element model to investigate prosthetic interface stresses of different posterior tibial slope. *Knee Surg Sports Traumatol Arthrosc.* 2015;23(11):3330–6.
27. Koh YG, Park KM, Kang K, Kim PS, Lee YH, Park KK, et al. Finite element analysis of the influence of the posterior tibial slope on mobile-bearing unicompartmental knee arthroplasty. *Knee.* 2021;29:116–25.
28. Suh DS, Kang KT, Son J, Kwon OR, Baek C, Koh YG. Computational study on the effect of malalignment of the tibial component on the biomechanics of total knee arthroplasty: a finite element analysis. *Bone Joint Res.* 2017;6(11):623–30.
29. Wünschel M, Leasure JM, Dalheimer P, Kraft N, Wülker N, Müller O. Differences in knee joint kinematics and forces after posterior cruciate retaining and stabilized total knee arthroplasty. *Knee.* 2013;20(6):416–21.
30. Wünschel M, Lo J, Dilger T, Wülker N, Müller O. Influence of bi- and tri-compartmental knee arthroplasty on the kinematics of the knee joint. *BMC Musculoskelet Disord.* 2011;27:12–29.
31. Liu F, Galvin A, Jin Z, Fisher J. A new formulation for the prediction of polyethylene wear in artificial hip joints. *Proc Inst Mech Eng H.* 2011;225(1):16–24.
32. Garabedian C, Bigerelle M, Najjar D, Migaud H. Wear pattern on a retrieved total knee replacement: the fourth body abrasion. *Biotribology.* 2017;11:29–43.
33. Rawal BR, Yadav A, Pare V. Life estimation of knee joint prosthesis by combined effect of fatigue and wear. *Procedia Technol.* 2016;23:60–7.

Publisher's Note

Springer Nature remains neutral with regard to jurisdictional claims in published maps and institutional affiliations.

Ready to submit your research? Choose BMC and benefit from:

- fast, convenient online submission
- thorough peer review by experienced researchers in your field
- rapid publication on acceptance
- support for research data, including large and complex data types
- gold Open Access which fosters wider collaboration and increased citations
- maximum visibility for your research: over 100M website views per year

At BMC, research is always in progress.

Learn more biomedcentral.com/submissions

